

ORIGINAL ARTICLE

Size-fraction partitioning of community gene transcription and nitrogen metabolism in a marine oxygen minimum zone

Sangita Ganesh^{1,3}, Laura A Bristow^{2,3}, Morten Larsen², Neha Sarode¹, Bo Thamdrup² and Frank J Stewart¹

¹*School of Biology, Georgia Institute of Technology, Atlanta, GA, USA* and ²*Department of Biology and Nordic Center for Earth Evolution (NordCEE), University of Southern Denmark, Odense, Denmark*

The genetic composition of marine microbial communities varies at the microscale between particle-associated (PA; > 1.6 μm) and free-living (FL; 0.2–1.6 μm) niches. It remains unclear, however, how metabolic activities differ between PA and FL fractions. We combined rate measurements with metatranscriptomics to quantify PA and FL microbial activity in the oxygen minimum zone (OMZ) of the Eastern Tropical North Pacific, focusing on dissimilatory processes of the nitrogen (N) cycle. Bacterial gene counts were 8- to 15-fold higher in the FL compared with the PA fraction. However, rates of all measured N cycle processes, excluding ammonia oxidation, declined significantly following particle (> 1.6 μm) removal. Without particles, rates of nitrate reduction to nitrite (1.5–9.4 nM N d^{-1}) fell to zero and N_2 production by denitrification (0.5–1.7 nM N d^{-1}) and anammox (0.3–1.9 nM N d^{-1}) declined by 53–85%. The proportional representation of major microbial taxa and N cycle gene transcripts in metatranscriptomes followed fraction-specific trends. Transcripts encoding nitrate reductase were uniform among PA and FL fractions, whereas anammox-associated transcripts were proportionately enriched up to 15-fold in the FL fraction. In contrast, transcripts encoding enzymes for N_2O and N_2 production by denitrification were enriched up to 28-fold in PA samples. These patterns suggest that the majority of N cycle activity, excluding N_2O and N_2 production by denitrification, is confined to a FL majority that is critically dependent on access to particles, likely as a source of organic carbon and inorganic N. Variable particle distributions may drive heterogeneity in N cycle activity and gene expression in OMZs.

The ISME Journal (2015) 9, 2682–2696; doi:10.1038/ismej.2015.44; published online 7 April 2015

Introduction

The genetic diversity and activity of pelagic marine microorganisms vary in complex patterns in response to environmental conditions and interspecies interactions. Such variation is best understood at the scale of meters, for example, over depth gradients of light or over regional (kilometer) gradients in nutrient availability. Microbial communities are also structured over much smaller spatial scales, notably the micron-scale distances separating free-living (FL) cells from those on the surfaces or within the diffusive boundary layer of suspended or sinking organic particles (Stocker, 2012). Extensive research has identified consistent taxonomic compositional differences between FL and particle-associated (PA) bacterial and archaeal communities (DeLong *et al.*, 1993; Hollibaugh *et al.*, 2000; Ganesh

et al., 2014), as well as differences in total microbial abundance, production and enzyme activity (Simon *et al.*, 2002; Grossart *et al.*, 2003, 2007). Surprisingly, most studies analyzing microbial genomic or metagenomic composition or rates of specific metabolic processes have either focused on microbes within a single biomass size fraction (typically the 0.2–3.0- μm range) or on bulk water samples. Such studies risk excluding important information about contributions from PA cells, larger non-PA cells or metabolic substrates in PA fractions. Furthermore, only a single study (Satinsky *et al.*, 2014) has examined community gene expression (metatranscriptomes) in PA versus FL communities. When coupled to measurements of metabolic rates, size-fractionated metatranscriptomics can help identify the drivers, magnitudes and spatial scales of biogeochemistry in the oceans.

The extent to which microbial metabolisms are partitioned between PA and FL communities remains uncharacterized for many ocean regions of importance to global biogeochemical cycles. These include the marine oxygen minimum zones (OMZs) where microbial communities control key steps in nitrogen (N), carbon and sulfur transformations. OMZs form in poorly ventilated regions where microbial respiration

Correspondence: FJ Stewart, School of Biology, Georgia Institute of Technology, Ford ES&T Building, Room 1242, 311 Ferst Drive, Atlanta, GA 30332, USA.

E-mail: frank.stewart@biology.gatech.edu

³These authors contributed equally to this work.

Received 23 October 2014; revised 11 February 2015; accepted 26 February 2015; published online 7 April 2015

fueled by high productivity in the overlying waters creates a layer of oxygen depletion. The largest OMZs occur in areas of persistent nutrient upwelling, as in the Eastern Tropical North Pacific (ETNP) off Mexico (Karstensen *et al.*, 2008). Encompassing $\sim 12 \times 10^6$ km² of shelf and off-shelf waters south of Baja California, the ETNP OMZ is the largest of the major permanent OMZs (41% of total OMZ area; Paulmier and Ruiz, 2009), with dissolved O₂ concentrations falling below the detection limit ($<0.1 \mu\text{M}$) at mid-water depths (~ 150 – 750 m; Cline and Richards, 1974; Tiano *et al.*, 2014).

Oxygen drawdown in OMZs significantly restructures the pelagic ecosystem, resulting in microbe-dominated communities expressing diverse micro-aerophilic or anaerobic metabolisms. These include the reductive processes of denitrification and anaerobic ammonia oxidation with nitrite (anammox), whose combined activity in OMZs contribute up to half of oceanic N loss as N₂ or N₂O gas (Codispoti *et al.*, 2001; Gruber, 2004). Research in the eastern Pacific OMZs, notably in the anoxic OMZ off Chile and Peru, indicates that anammox and denitrification are linked to varying degrees with a diverse set of other microbial N transformations, including the production of nitrite and nitrate via nitrification along the oxycline and dissimilatory nitrate reduction to ammonium within the OMZ (Lam *et al.*, 2009; Kalvelage *et al.*, 2013). OMZ N cycle processes also mediate key steps in other elemental cycles, for example, the fixation of carbon by anammox and nitrifying autotrophs, the remineralization of organic carbon and nutrients by denitrifying heterotrophs, and the oxidation of reduced sulfur compounds by chemoautotrophic denitrifiers (Ulloa *et al.*, 2012).

The distributions of these networked metabolic interactions at multiple spatial scales are becoming understandable for some OMZs. Surveys combining marker gene counts and rate measurements have suggested mesoscale patterns in N cycling along coastal to offshore gradients in the Eastern Tropical South Pacific (ETSP) OMZ off Chile and Peru (Kalvelage *et al.*, 2013), as well as clear depth-specific variation in N cycle genes, transcripts, and rates (Thamdrup *et al.*, 2006; Dalsgaard *et al.*, 2012; Stewart *et al.*, 2012). Recently, analysis of microbial metagenomes in the ETSP OMZ also identified a non-uniform distribution of N cycle genes among filter size fractions (Ganesh *et al.*, 2014). Genes for aerobic ammonia oxidation at OMZ boundaries and for anammox at the OMZ core were consistently overrepresented in the FL fraction (0.2– $1.6 \mu\text{m}$). In contrast, genes mediating different steps of denitrification showed variable distributions between size fractions. Genes encoding NarG, part of the enzyme catalyzing nitrate reduction to nitrite, were abundant and evenly distributed between PA ($>1.6 \mu\text{m}$) and FL fractions within the OMZ, whereas genes mediating the two terminal steps of denitrification, the reduction of nitric oxide to nitrous oxide (*norB*) and nitrous oxide to dinitrogen (*nosZ*), exhibited a

fourfold increase in relative abundance in PA compared with FL metagenomes. These data highlight a potential separation of linked metabolic processes at varying spatial scales, potentially over micron gradients separating PA and FL communities.

The proportional contribution of PA N metabolism to bulk process rates in OMZs remains unclear, notably for the larger ETNP OMZ. Despite recent studies describing the diversity and activity of key functional taxonomic groups in the ETNP (Podlaska *et al.*, 2012; Rush *et al.*, 2012; Beman *et al.*, 2012, 2013), this region remains under-explored from a microbiological and molecular perspective. Assessing the actual biochemical significance of microspatial separation of microbial processes in OMZs requires quantification of metabolic rates and gene expression among size fractions from diverse OMZ regions. We combine community transcription profiling and rate measurements to quantify size fraction partitioning of key steps of the marine N cycle. These data, coupled with taxonomic analysis of genes and transcripts and estimates of bacteria abundance among size fractions, indicate a significant contribution of particles and PA bacteria to OMZ N cycling.

Materials and methods

Molecular analysis

Sample collection. Samples were collected from the ETNP OMZ during the OMZ Microbial Biogeochemistry Expedition cruise (*R/V New Horizon*, 13–28 June 2013). Seawater was sampled from six depths spanning the upper oxycline (30 m), lower oxycline (85 m) oxic–nitrite interface (91 m), secondary chlorophyll maximum (100 m), secondary nitrite maximum (125 m) and OMZ core (300 m) at Station 6 (18° 54.0' N, 104° 54.0' W) on 19 June. Collections were made using Niskin bottles on a rosette containing a Conductivity Temperature Depth profiler (Sea-Bird SBE 911plus, Sea-Bird Electronics Inc., Bellevue, WA, USA) equipped with a Seapoint fluorometer (Seapoint Sensors Inc., Exeter, NH, USA) and SBE43-dissolved oxygen sensor (Sea-Bird Electronics Inc.). High-resolution Switchable Trace amount OXYgen sensors (STOX) were also mounted to the rosette to quantify oxygen at nanomolar concentrations (Revsbech *et al.*, 2009; Supplementary Methods). Samples were also collected from 20, 40, 90, 100, 125 and 300 m during a replicate cast on the same day and used to count bacterial 16S rRNA genes.

Size-fractionated biomass was collected for RNA analysis by sequential inline filtration of seawater (~ 10 – 15 l) through a nylon disk filter (47 mm, 30 μm pore size, Millipore, Bellerica, MA, USA), a glass fiber disc filter (GF/A, 47 mm, 1.6 μm pore size, Whatman, GE Healthcare Bio-sciences, Pittsburgh, PA, USA) and a primary collection filter (Sterivex, 0.22 μm pore size, Millipore) via peristaltic pump. Replicate filters for DNA were collected from

equivalent water volumes following RNA collection. Water samples (45 ml each) for 16S rRNA gene counts were filtered through 0.2 µm disc filters (25 mm, cellulose nitrate, Whatman). Disc filters were transferred to cryovials containing RNA stabilizing buffer (25 mM sodium citrate, 10 mM EDTA and 70 g ammonium sulfate per 100 ml solution, pH 5.2) for RNA samples or lysis buffer (50 mM Tris-HCl, 40 mM EDTA and 0.73 M sucrose) for DNA samples. Sterivex filters were filled with either RNA stabilizing buffer or lysis buffer, capped and flash-frozen (RNA samples). Filters were stored at -80 °C. Less than 20 min elapsed between sample collection (water on deck) and fixation in buffer.

DNA and RNA extraction. DNA was extracted from disc and Sterivex filters using a phenol/chloroform protocol as in Ganesh *et al.* (2014). Cells were lysed by adding lysozyme (2 mg in 40 µl of lysis buffer per filter) directly to the disc filter containing cryovial or to the Sterivex cartridge, sealing the caps/ends and incubating for 45 min at 37 °C. Proteinase K (1 mg in 100 µl lysis buffer with 100 µl 20% SDS) was added, and cryovials and cartridges were resealed and incubated for 2 h at 55 °C. The lysate was removed and DNA was extracted once with phenol:chloroform:isoamyl alcohol (25:24:1) and once with chloroform:isoamyl alcohol (24:1), and then concentrated by spin dialysis using Ultra-4 (100 kDa, Amicon, Millipore) centrifugal filters.

RNA was extracted from disc and Sterivex filters using a modification of the *mirVana* miRNA Isolation kit (Ambion, Life Technologies, Carlsbad, CA, USA) as in Stewart *et al.* (2012). Filters were thawed on ice and RNA stabilizing buffer was removed by pipette from cryovials or expelled via syringe from Sterivex cartridges and discarded. Cells were lysed by adding lysis buffer and miRNA homogenate additive (Ambion) directly to the cryovial or cartridge. Following vortexing and incubation on ice, lysates were transferred to RNase-free tubes and processed via acid-phenol/chloroform extraction according to the kit protocol. The TURBO DNA-free kit (Ambion) was used to remove DNA and the extract was purified using the RNeasy MinElute Cleanup Kit (Qiagen, Hilden, Germany).

16S rRNA gene counts. Quantitative PCR was used to count bacterial 16S rRNA genes in bulk seawater (biomass >0.2 µm) and in 0.2–1.6 and 1.6–30 µm size fractions. Extracts from the >30 µm fraction did not contain measureable DNA (via Qubit) and failed to yield signals during quantitative PCR with diluted and undiluted extracts. We were not able to sum counts from size-fractionated samples to obtain counts per volume because exact volumes of filtered seawater were not recorded. We instead used samples of fixed volume from a replicate cast ('Sample collection' section above) to quantify total gene copies per ml of seawater. Because equal water volumes passed through sequential filters during

size fractionation, counts from size-fractionated samples were used to quantify the ratio of copies in the 0.2–1.6-µm fraction to those in the 1.6–30-µm fraction (FL/PA ratio); counts from the >30 µm fraction are assumed to be negligible.

Quantitative PCR used TaqMan-based reagents and universal bacterial 16S primers 1055 f and 1392r, as in Ritalahti *et al.* (2006) and Hatt *et al.* (2013). Tenfold serial dilutions of DNA from a plasmid carrying a single copy of the 16S rRNA gene (from *Dehalococcoides mccartyi*; Ritalahti *et al.*, 2006) were included on each quantitative PCR plate and used to generate standard curves. Assays were run on a 7500 Fast PCR System and a StepOnePlus Real-Time PCR System (Applied Biosystems, Life Technologies). All samples were run in triplicate (20 µl each) and included 1× TaqMan Universal PCR Master Mix (Life Technologies), 300 nM of primers, 300 nM of TaqMan MGB probe (Life Technologies) and 2 µl of template DNA. Thermal cycling involved incubation at 50 °C for 2 min to activate uracil-N-glycosylase, followed by 95 °C for 10 min to inactivate uracil-N-glycosylase, denature template DNA and activate the AmpliTaq Gold polymerase, followed by 40 cycles of denaturation at 95 °C (15 s) and annealing at 60 °C (1 min).

16S rRNA gene amplicon sequencing. High-throughput sequencing of dual-indexed PCR amplicons encompassing the V4 region of the 16S rRNA gene was used to assess bacterial community composition in all filter fractions. Despite low DNA yields (above), 16S gene fragments were amplifiable from the >30-µm fraction. The diversity of amplicons generated using Archaea-specific primers was not evaluated. Amplicons were synthesized using Platinum PCR SuperMix (Life Technologies) with primers F515 and R806 (Caporaso *et al.*, 2011). Both forward and reverse primers were barcoded and appended with Illumina-specific adapters according to Kozich *et al.* (2013). Thermal cycling involved: denaturation at 94 °C (3 min), followed by 30 cycles of denaturation at 94 °C (45 s), primer annealing at 55 °C (45 s) and primer extension at 72 °C (90 s), followed by extension at 72 °C for 10 min. Amplicons were analyzed by gel electrophoresis to verify size (~400 bp) and purified using the QIAquick PCR Clean-Up Kit (Qiagen). Amplicons from different samples were pooled at equimolar concentrations and sequenced on an Illumina MiSeq (Illumina, San Diego, CA, USA) using a 500 cycle kit with 5% PhiX as a control.

cDNA synthesis and metatranscriptome sequencing Shotgun Illumina sequencing of community cDNA was used to characterize gene expression in 0.2–1.6 µm and 1.6–30 µm biomass fractions. Most samples of the >30-µm fraction did not yield sufficient RNA for sequencing; this fraction was excluded from meta-omic analysis. Community RNA

was prepared for sequencing using the ScriptSeq v2 RNA-Seq Library preparation kit (Epicenter, Madison, WI, USA). Briefly, cDNA was synthesized from fragmented total RNA (rRNA was not removed) using reverse transcriptase and amplified and barcoded using ScriptSeq Index PCR Primers (Epicenter) to generate single-indexed cDNA libraries. cDNA libraries were pooled and sequenced on an Illumina MiSeq using a 500 cycle kit (Supplementary Table S1). Metagenomes from coupled DNA samples were analyzed to allow standardization of taxon transcript levels relative to abundance in the DNA pool. These data sets were generated in a separate study (in review, NCBI accession SRP044185) using the Nextera XT DNA Sample Prep kit and paired-end MiSeq sequencing as above for cDNA samples.

Sequence analysis—16S rRNA gene amplicons

Amplicons were analyzed using QIIME (Caporaso *et al.*, 2010) following standard protocols. Barcoded sequences were de-multiplexed and filtered to remove low-quality reads (Phred score <25). Paired-end sequences were merged using custom scripts incorporating the FASTX toolkit (http://hannonlab.cshl.edu/fastx_toolkit/index.html) and USEARCH algorithm (Edgar, 2010), with criteria of minimum 10% overlap and 95% nucleotide identity within the overlapping region. Merged sequences were clustered into operational taxonomic units at 97% sequence similarity using open-reference picking with the UCLUST algorithm (Edgar, 2010), with taxonomy assigned to representative operational taxonomic units from each cluster using the Greengenes database (DeSantis *et al.*, 2006). Operational taxonomic unit counts were rarefied (10 iterations) and alpha diversity was quantified at a uniform sequence depth ($n=6506$) using the phylogenetic diversity metric of Faith (1992). To compare community composition between samples, sequences were aligned using the PyNAST aligner (Caporaso *et al.*, 2010) and beta diversity was calculated using the weighted Unifrac metric (Lozupone and Knight, 2005). Sample relatedness based on Unifrac was visualized with a two-dimensional principal coordinate analysis.

Sequence analysis—metatranscriptomes and metagenomes

Analysis of protein-coding genes and transcripts followed that of Stewart *et al.* (2012) and Ganesh *et al.* (2014). Reads were filtered by quality and merged as described above. rRNA transcripts were identified using riboPicker (Schmieder *et al.*, 2012) and removed. Merged non-rRNA sequences were queried via BLASTX against the NCBI-nr database (November 2013). BLASTX matches to bacterial and archaeal genes (>bit score 50) were retained to evaluate marker genes of dissimilatory N metabolism: ammonia monooxygenase (*amoC*), nitrite oxidoreductase (*nxrB*), hydrazine oxidoreductase (*hzo*), nitrate

reductase (*narG*), nitrite reductase (*nirK+nirS*), nitric oxide reductase (*norB*) and nitrous oxide reductase (*nosZ*). N gene transcript abundances were normalized based on gene length and expressed as a proportion of the abundance of transcripts matching the gene encoding RNA polymerase subunit B (*rpoB*), as has been done in studies of diverse bacteria (for example, Schumann *et al.*, 2010; Ceja-Navarro *et al.*, 2014; Dalsgaard *et al.*, 2014; Eldholm *et al.*, 2014). Although *rpoB* expression can vary (Vandecasteele *et al.*, 2001), *rpoB* appears to be one of the more stably expressed housekeeping genes (Sue *et al.*, 2004; Sihto *et al.*, 2014). Furthermore, it has been shown that *rpoB* can be a proxy of bulk mRNA transcription level for bacteria (Milohanic *et al.*, 2003; Sue *et al.*, 2004)—*rpoB*-normalized values therefore reflect transcription of a target gene relative to a housekeeping gene under a given condition/sample.

The taxonomic composition of protein-coding genes and transcripts was determined using MEta-Genome ANalyzer 5 (Huson *et al.*, 2011) based on the annotations of BLASTX-identified genes, according to the NCBI taxonomy. The proportional contribution of a taxon (Phyla and Class levels) to the RNA pool was calculated as an RNA:DNA ratio, calculated as in Frias-Lopez *et al.* (2008) and Stewart *et al.* (2012) to account for variation in taxon abundance in the DNA pool: (protein-coding RNA reads per taxon/total protein-coding RNA reads)/(protein-coding DNA reads per taxon/total protein-coding DNA reads). For subsets of transcripts matching specific functional taxa (anammox genera, *Nitrospina*), genes differentially expressed between FL and PA fractions were identified using baySeq (Hardcastle and Kelly, 2010) as in Ganesh *et al.* (2014). Full details regarding sequence analysis are in the Supplementary Methods.

Amplicon and metatranscriptome sequences are available through NCBI under BioProject ID PRJNA263621

Biochemical analysis. Water for rate measurements was taken from Niskin bottles immediately after arrival on deck and transferred to 2 l glass bottles. Bottles were overflowed (three volume equivalents) and sealed without bubbles using deoxygenated butyl rubber stoppers (De Brabandere *et al.*, 2014). Bottles were stored in the dark at *in situ* temperature until experimentation (<6 h). Each bottle was purged with a gas mixture of helium and carbon dioxide (800 p.p.m. carbon dioxide) for ~20 min. Under a slight overpressure, water was dispensed into 12 ml exetainers (Labco, Lampeter, Ceredigion, UK) either directly or through helium-flushed inline filter holders, and immediately capped with deoxygenated lids.

Rates were measured for two biomass fractions: bulk water containing all particles (no filtration) and water without particles >1.6 μm . Particles were excluded via filtration as described above. Exetainers

were subsequently amended with ^{15}N -labeled substrate by injection through the septum. Three ^{15}N amendments were carried out for all samples: $^{15}\text{NH}_4^+$ addition (to $5\ \mu\text{M}$ concentration), $^{15}\text{NO}_2^-$ addition ($5\ \mu\text{M}$) and $^{15}\text{NO}_3^-$ addition ($15\ \mu\text{M}$). Headspaces of 2 ml were introduced into each exetainer and flushed twice with the helium–carbon dioxide mixture as in De Brabandere *et al.* (2014). For each experiment, triplicate exetainers were preserved with $100\ \mu\text{l}$ of 50% (w/v) ZnCl_2 at the start of the incubation and again at the end point (27 h). Oxygen concentration was $<80\ \text{nM}$ in all treatments. The act of filtering did not affect exetainer oxygen content (Supplementary Methods).

The production of $^{14}\text{N}^{15}\text{N}$ and $^{15}\text{N}^{15}\text{N}$ was determined on a gas chromatography isotope ratio mass spectrometer as in Dalsgaard *et al.* (2012). Rates of N_2 production by anammox and denitrification were calculated using the equations in Thamdrup and Dalsgaard (2002). Nitrite oxidation was determined from the production of $^{15}\text{NO}_3^-$ from incubations with $^{15}\text{NO}_2^-$. After removal of unused $^{15}\text{NO}_2^-$ using sulfamic acid, $^{15}\text{NO}_3^-$ was converted to $^{15}\text{NO}_2^-$ with cadmium and then to N_2 with sulfamic acid (Füssel *et al.*, 2012; McIlvin and Altabet 2005). Ammonia oxidation and nitrate reduction rates were determined as production of $^{15}\text{NO}_2^-$ from incubations with $^{15}\text{NH}_4^+$ or $^{15}\text{NO}_3^-$. $^{15}\text{NO}_2^-$ produced during incubations was converted to N_2 with sulfamic acid. N_2 was then analyzed on the gas chromatography isotope ratio mass spectrometer. Rates for all processes were calculated from the slope of the linear regression of $^{14}\text{N}^{15}\text{N}$ or $^{15}\text{N}^{15}\text{N}$ with time. *T*-tests were applied to determine whether rates were significantly different from zero ($P < 0.05$). Non-significant rates are presented as not detected.

Nitrate, nitrite and ammonium concentrations were determined using standard protocols, as described in the Supplementary Methods. The N deficit estimates the amount of fixed N loss and was calculated as: $\text{N deficit} = (\text{DIN}) - (16 \times [\text{PO}_4^{3-}] \times 0.86)$, where $\text{DIN} = [\text{NO}_3^-] + [\text{NO}_2^-] + [\text{NH}_4^+]$. The value of 0.86 accounts for the release of PO_4^{3-} from organic N remineralized during denitrification (Codispoti *et al.*, 2001).

Results and discussion

Particle removal significantly altered N cycle rates and gene expression, suggesting physiological variation at the microscale between water column and PA niches. These patterns are discussed below relative to oxygen and N concentrations, bacterial abundance and community taxonomic composition.

Oxygen and nitrogen

Oxygen concentrations recorded by the SBE43 sensor were highest ($\sim 200\ \mu\text{M}$) in surface waters and declined steeply in the oxycline between 30 and 85 m (Figure 1a). From 90 to 800 m, concentrations measured by STOX sensors were $<50\ \text{nM}$, with

the majority close to or below the detection limit (Figure 1b) representing the OMZ core. Oxygen concentrations at the six depths sampled for size fractionation work varied markedly, from $200\ \mu\text{M}$ at 30 m to $229\ \text{nM}$ at 85 m, representing the upper and lower limits of the oxycline, respectively, $43\ \text{nM}$ at the oxic–nitrite interface (91 m), $21\ \text{nM}$ at the secondary chlorophyll maximum (100 m) and $14\ \text{nM}$ at the secondary nitrite maximum (125 m), before reaching the detection limit ($9\ \text{nM}$) at 150 m and staying undetectable to 300 m in the OMZ core (Figure 1b). Oxygen profiles coincided with patterns in nitrate, nitrite and the N deficit. As commonly observed in anoxic OMZs (Ulloa *et al.*, 2012), a prominent secondary nitrite maximum (up to $6.1\ \mu\text{M}$) was observed as oxygen declined, coinciding with local nitrate and N deficit minima (Figures 1a and c). Ammonium concentrations remained below $155\ \text{nM}$ throughout the profile. Chlorophyll peaked at 0.6 and $0.8\ \mu\text{g l}^{-1}$ at 50 and 100 m, respectively, indicating the primary and secondary chlorophyll maxima characteristic of OMZs (Figure 1c; Ulloa *et al.*, 2012).

16S rRNA gene abundance

Counts of bacterial 16S rRNA genes varied by an order of magnitude with depth (Figure 1f). Bulk seawater counts declined from $\sim 6 \times 10^5$ per ml in the primary chlorophyll maximum and upper oxycline to 1.3×10^5 at the oxic–nitrite interface (90 m), before increasing to a maximum of 1.4×10^6 at the OMZ core. This pattern agrees with trends from other OMZ sites, where particulate backscattering and bacterial load show local maxima in the photic zone and again in the OMZ (Spinrad *et al.*, 1989; Naqvi *et al.*, 1993; Whitmire *et al.*, 2009). At all depths, gene numbers were substantially higher in the 0.2– $1.6\ \mu\text{m}$ (FL) fraction compared with the 1.6 – $30\ \mu\text{m}$ (PA) fraction, with FL/PA ratios from 8 to 15 (Figure 1f). Elevated microbial biomass in FL compared with PA fractions has been observed in diverse ocean regions (Cho and Azam 1988; Karl *et al.*, 1988; Turley and Stutt 2000; Ghiglione *et al.*, 2009). Here, FL/PA was lowest at 300 m, suggesting an increased contribution of PA or large bacteria within the OMZ core, possibly related to increases in particle load or size.

Community composition—16S rRNA gene amplicons

Community 16S rRNA gene diversity varied substantially among biomass fractions and depths. Unifrac-based clustering indicated that size class was a stronger predictor of community relatedness compared with depth, notably for samples from the OMZ layer (100, 125 and 300 m) (Figure 2). Phylogenetic diversity differed widely among fractions, with values in the two PA fractions up to 50% greater than those for the corresponding FL fraction (Supplementary Figure S1). Elevated diversity in PA communities has been reported for the ETSP OMZ

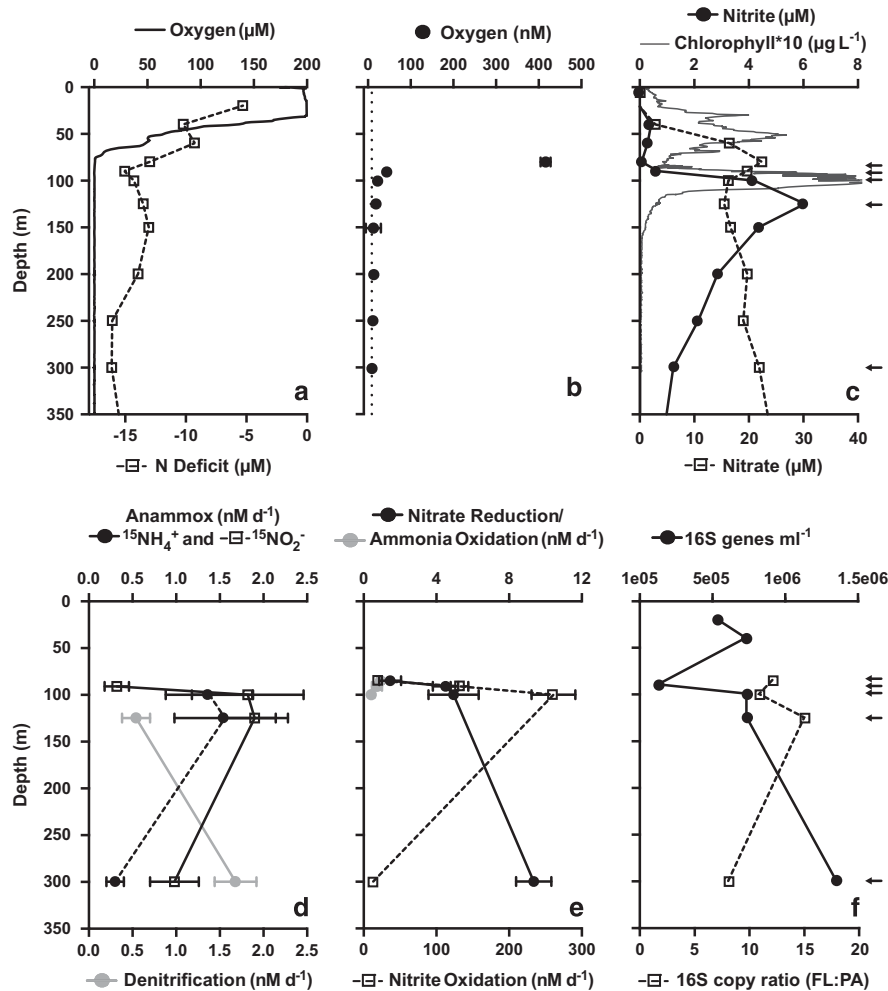


Figure 1 Vertical profiles of hydrochemical parameters, bulk N cycling process rates and bacterial 16S rRNA gene counts at Station 6, off Manzanillo, Mexico on 19 June 2013. The N deficit (**a**, open squares) is shown relative to oxygen concentrations, measured during the upcast profile with both a SBE43 sensor (**a**; solid line) and STOX sensors (**b**), and to profiles of nitrite, nitrate and chlorophyll concentration (**c**). The dashed line in **b** indicates the detection limit of the STOX sensors (~9 nM). N cycle process rates (**d**, **e**) are bulk rates (no size fractionation) in mM N per day. (**f**) Quantitative PCR-based counts of 16S rRNA gene copies per ml of bulk seawater (all biomass >0.2 µm) and the ratio of gene counts in the FL (0.2–1.6 µm) biomass fraction to counts in the PA (1.6–30 µm) fraction. Arrows (**c**, **f**) indicate the depths sampled for rate measurements. Error bars represent the standard error.

(Ganesh *et al.*, 2014) and may be driven by increased niche richness due to substrate heterogeneity on particles, or to the exposure of particles during sinking to diverse communities in different biogeochemical zones. Here, phylogenetic diversity in all size fractions peaked at the secondary chlorophyll maximum, similar to trends reported for non-fractionated samples (biomass >0.2 µm) from ETNP sites north of the study area, where taxon richness peaked just below the oxycline, before declining with depth (Beman and Carolan, 2013). That study identified deoxygenation as a driver of bulk community diversity, whereas our results suggest that diversity estimates vary depending on the filter fraction examined.

Several microbial clades with roles in N cycling were proportionally enriched in FL relative to PA fractions (Figure 3; Supplementary Figure S2).

Sequences matching ammonia-oxidizing Thaumarchaeota and nitrite-oxidizing *Nitrospina* (classified as Deltaproteobacteria in Supplementary Figure S3; Teske *et al.*, 1994) peaked in relative abundance (2.2–2.9% of total) in the FL fraction from the lower oxycline before declining with depth. Abundances of both groups decreased by 50–60% in the 1.6–30-µm PA fraction relative to the FL fraction and were negligible in the >30-µm PA fraction. Sequences matching the anammox Planctomycete *Candidatus Scalindua* (Order Brocadiales) were also confined primarily to the FL fraction, peaking at 14.1% of total FL amplicons at 300 m, compared with 0.3–1.5% in PA fractions. Anammox bacteria were previously shown to be enriched in the smallest size fractions in studies of the Chilean OMZ (Ganesh *et al.*, 2014), the Black Sea (Fuchsman *et al.*, 2012), and an OMZ off Costa Rica (Kong *et al.*, 2013), but have also been

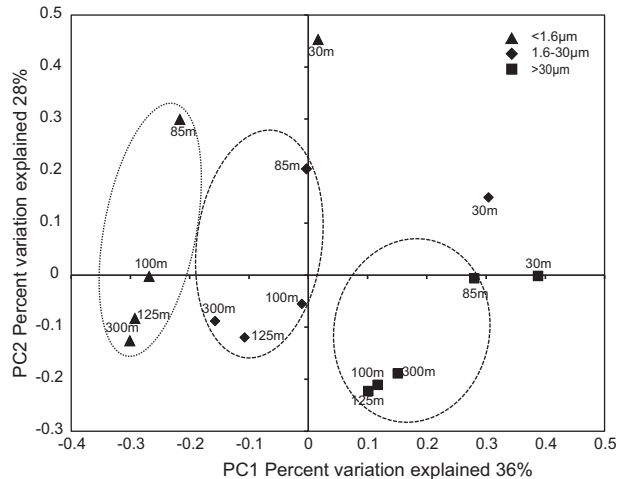


Figure 2 Principle coordinate analysis of community taxonomic relatedness based on 16S rRNA gene amplicons, as quantified by the weighted Unifrac metric. Samples from different filter size fractions are circled (excluding outliers from the 30-m depth).

detected in direct contact with particles in oxygen-depleted waters over the Namibian shelf (Woebken *et al.*, 2007).

The composition of the ETNP bacterial community with potential roles in coupled N and sulfur cycles differed from that of other OMZs and varied among size fractions. The sulfur-oxidizing and denitrifying Gammaproteobacterial SUP05 clade, a ubiquitous inhabitant of low-oxygen waters (Wright *et al.*, 2012), accounted for <0.2% of amplicons in ETNP samples. ETNP samples were instead enriched in members of the uncultured SAR406 and Deltaproteobacterial SAR324 lineages (Figure 3), as well as Gammaproteobacteria of the Thiohalorhabdales, Chromatiales and Thiotrichales (Supplementary Figure S3 and Supplementary Information), all of which may contain sulfur-oxidizing members. The SAR406 cluster was particularly abundant in FL samples, contributing 22% (average) of FL sequences, compared with 2.8% in PA fractions (Figure 3). SAR406 may participate in sulfur cycling via dissimilatory polysulfide reduction to sulfide or sulfide oxidation (Wright *et al.*, 2014), although pathways for denitrification and carbon fixation have not been unambiguously identified. The SAR324 lineage, which includes members with genes for sulfur chemolithoautotrophy and nitrite reduction (Swan *et al.*, 2011; Sheik *et al.*, 2014), was also enriched in FL samples, representing 5–8% of sequences at OMZ depths, compared with <0.5% in PA fractions (Supplementary Figure S3). FL enrichment of SAR406 and SAR324 is consistent with an autotrophic lifestyle, as autotrophs would not require organic particles for carbon acquisition. Whereas sulfide-oxidizing autotrophs in other OMZs are capable of using oxidized N compounds as terminal oxidants (Walsh *et al.*, 2009; Canfield *et al.*, 2010), the

extent to which ETNP clades participate in sulfur-driven denitrification remains unclear.

Many microbial groups common to low-oxygen waters, including those discussed above, were either at low abundance or absent from the >30- μm PA fraction. This fraction was instead enriched in taxa known to associate with the surfaces or guts of plankton or polymer aggregates (for example, fecal pellets), notably Gammaproteobacteria related to *Vibrio*, *Pseudomonas* and *Alteromonas* (Supplementary Figure S3; Rao *et al.*, 2005; Hunt *et al.*, 2008; Ivars-Martinez *et al.*, 2008). Microorganisms on particles >30 μm are likely a minor component of the bulk OMZ microbial community, and may be relatively transient members, passing through low-oxygen depths attached to sinking aggregates or zooplankton.

RNA:DNA ratios

The taxonomic identities of protein-coding genes and transcripts suggest differences in the proportional contributions of specific taxa to bulk transcript pools in FL versus PA (1.6–30 μm) communities. RNA/DNA ratios for several groups with roles in N cycling, including anammox bacteria (Brocadiales), ammonia-oxidizing Thaumarchaeota and nitrite-oxidizing *Nitrospina* bacteria, were consistently elevated in FL relative to PA communities (Figure 4). These groups were also proportionately enriched in 16S gene pools from FL samples. In contrast, groups such as the Actinobacteria and Gammaproteobacteria exhibited greater RNA/DNA ratios in the PA fraction. Similar patterns were observed for ratios based on 16S rRNA gene amplicons and transcripts from metatranscriptomes (rRNA:rDNA; Supplementary Figure S4). Although RNA:DNA ratios, based either on target genes or community gene pools, have been used as proxies for metabolic activity (Campbell and Yu, 2011; Hunt *et al.*, 2013; Satinsky *et al.*, 2014), linking ratios to activity is tenuous. Notably, as RNA/DNA ratios are based on proportional abundances, increases in taxon representation in the transcriptome can reflect either increases in the activity of the target taxon or decreases in the activity of other organisms. Furthermore, using ratios to infer activity is challenging for broad divisions such as the Gammaproteobacteria that contain taxonomically and functionally diverse members, as the relationship between cell RNA content and activity is unlikely to be consistent across members or activity gradients (Blazewicz *et al.*, 2013). Here, the composition of Gammaproteobacteria at the Order level varied widely (Supplementary Figure S3), highlighting the possibility that taxon-specific differences confounds interpretation of Phylum-level ratios. Studies at finer levels of taxonomic resolution utilizing transcriptome mapping to reference genomes coupled with measurements of absolute transcript numbers are necessary to confirm shifts in taxon-specific activity between FL and PA niches. The latter could reflect differences in substrate conditions or the proportions of live versus dead cells between fractions.

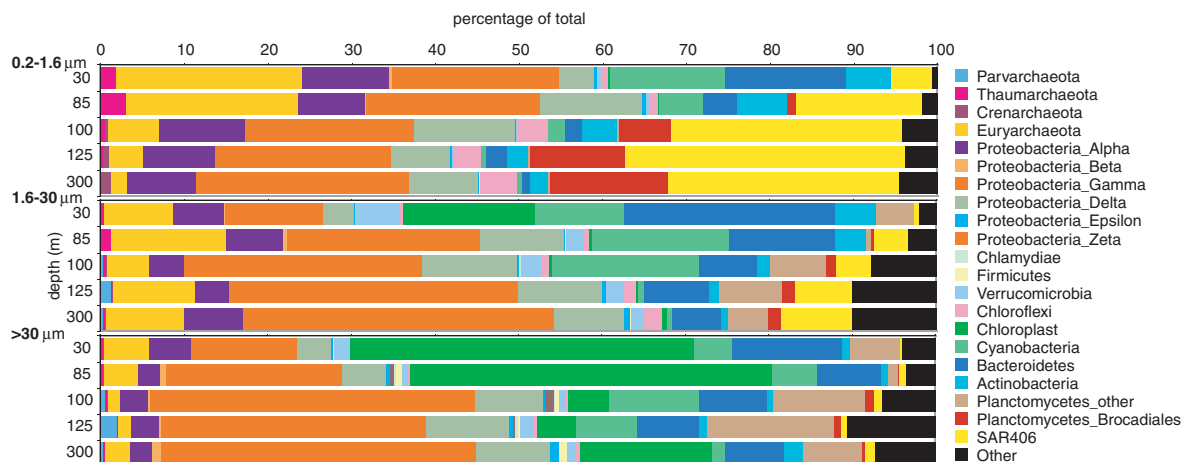


Figure 3 ETNP OMZ bacterial community diversity revealed by 16S rRNA gene Illumina sequencing. The abundances of major bacterial divisions are shown as a percentage of total identifiable 16S rRNA gene sequences. ‘Other’ includes 34 divisions, including unassigned sequences.

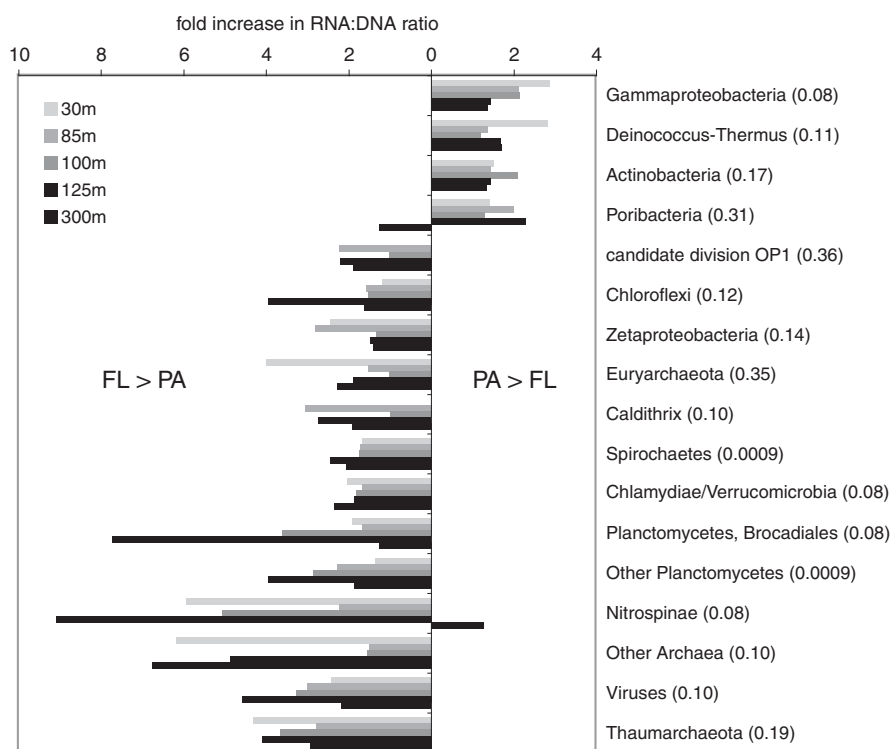


Figure 4 Fold increase in taxon RNA/DNA ratios between PA (1.6–30 μm) and FL (0.2–1.6 μm) communities. Plot shows the fold increase in ratios for major taxonomic groups identified by the NCBI annotations of protein-coding genes and transcripts in coupled metatranscriptome and metagenome data sets. Values right of zero indicate higher ratios in PA communities (PA/FL > 1). Values left of zero indicate higher ratios in FL communities (FL/PA > 1). The plot shows only groups with relative abundance in metagenome data sets greater than 0.2% of total sequences, and only groups with an average (across all five depths) fold increase > 1.5. Numbers in parentheses are false discovery rate q -values for t -test comparisons of PL and FL ratios, calculated as in Storey and Tibshirani (2003).

Bulk biochemical rates

N transformation rates in bulk water (no filter fractionation) varied among processes and over depth gradients. Rates of nitrate reduction to nitrite increased with depth and diminishing *in situ* oxygen concentration, with measured rates from 1.5 to 9.4 nM N d^{-1} (Figure 1e). The reduction of nitrite to N_2 via denitrification was slower and measurable only

below 125 m, with a maximum of 1.7 nM N d^{-1} at 300 m (Figure 1d). Anammox was measurable between 91 and 300 m at rates from 0.3 to 1.9 nM N d^{-1} , with the highest rates in the secondary nitrite maximum. Anammox rates after $^{15}\text{NO}_2^-$ addition were consistently higher than those after $^{15}\text{NH}_4^+$ addition, similar to trends in De Brabandere *et al.* (2014) working in the ETSP OMZ. The largest discrepancy in $^{15}\text{NO}_2^-$

versus $^{15}\text{NH}_4^+$ -based anammox rates occurred at 300 m, the depth where maximum denitrification rates were measured (Figure 1d), suggesting that nitrite shunting by denitrifiers could explain the offset in anammox rates, as proposed by De Brabandere *et al.* (2014). In this interpretation, incubations with $^{15}\text{NH}_4^+$ reflect true anammox rates, while incubations with $^{15}\text{NO}_2^-$ overestimate the process. Our measured N loss rates are similar to those reported by Babbin *et al.* (2014) for stations close to ours (0.8–4.7 and 0.9–3.3 nmN d^{-1} for anammox and denitrification, respectively), and are generally consistent with those recorded in other OMZs (Lam and Kuypers, 2011). Dissimilatory nitrate reduction to ammonium was not detected in any of the samples. Ammonia oxidation was detected only at 100 m or shallower, with maximum rates at 85 m (0.92 nmN d^{-1}), the shallowest and most oxygenated of the depths where rates were measured (Figure 1e). These rates are at the lower end of those previously observed in the Gulf of California and ETNP (0–348 nmN d^{-1} ; Beman *et al.*, 2012) and in the ETSP OMZ (0.2–89 nmN d^{-1} ; Kalvelage *et al.*, 2013). Nitrite oxidation was detected at all depths except 125 m, at rates (13–261 nmN d^{-1} ; Figure 1e) up to an order of magnitude higher than those for other processes, with rates peaking in the secondary chlorophyll maximum, suggesting a decoupling between ammonia and nitrite oxidation. These values are consistent with nitrite oxidation rates measured in the Gulf of California and ETNP (0–213 nmN d^{-1} ; Beman *et al.*, 2013), the ETSP (5–928 nmN d^{-1} ; Kalvelage *et al.*, 2013) and the Benguela upwelling (14–372 nmN d^{-1} ; Füssel *et al.*, 2012), further confirming the activity of nitrite oxidizers at nanomolar oxygen levels (Füssel *et al.*, 2012).

Size-fractionated biochemical rates and gene expression

Nitrate reduction and denitrification. Rates of nitrate reduction to nitrite were undetectable after removal of particles ($>1.6 \mu\text{m}$) by filtration (Figure 5a). Filtration therefore removed either a significant proportion of total nitrate-reducing cells or a critical substrate source fueling FL nitrate

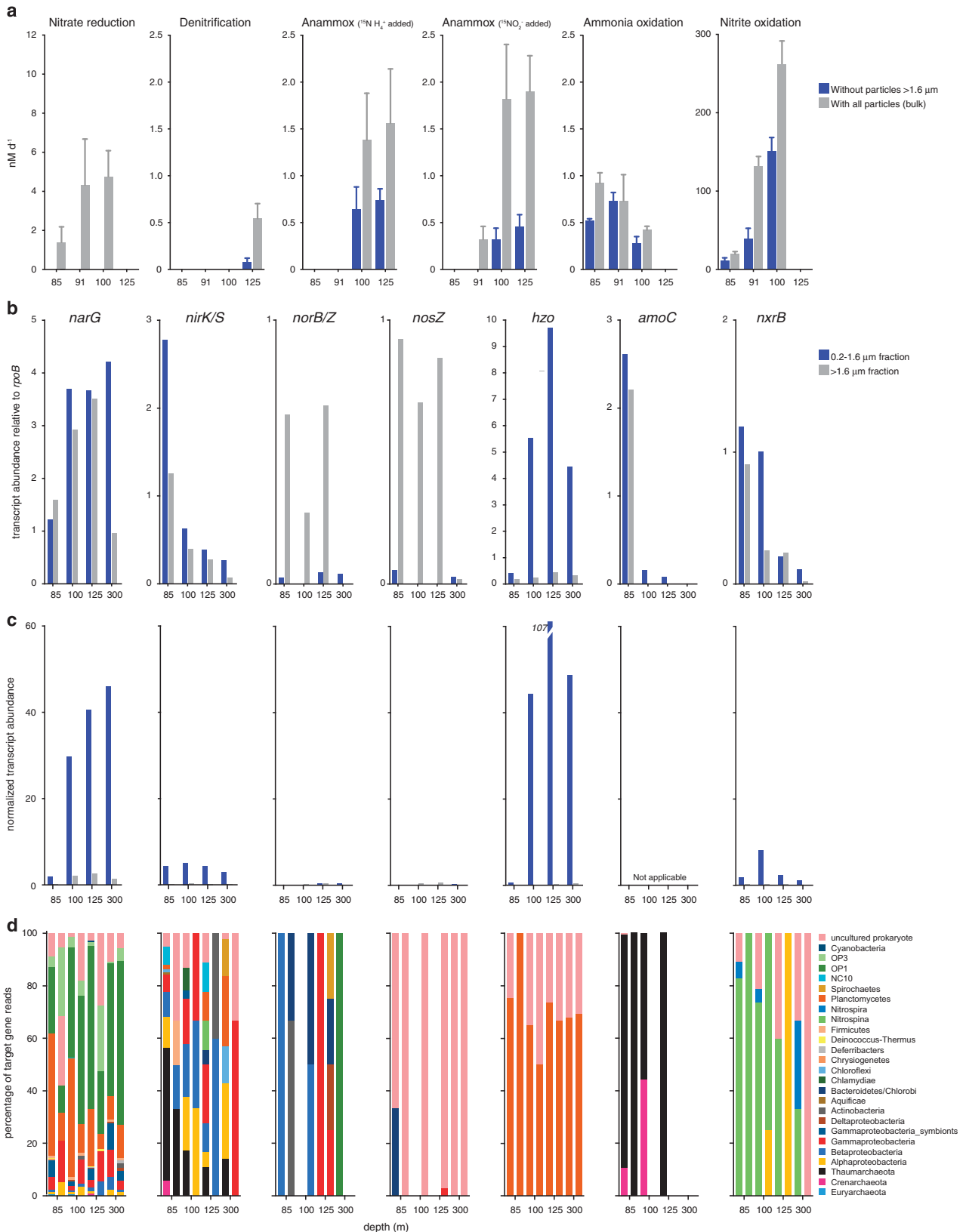
reducers. Although the proportional abundances of transcripts encoding nitrate reductase (*narG*) were uniform among filter fractions (Figure 5b), suggesting roughly equivalent contributions of nitrate reduction to fraction-specific metabolism in PA and FL niches, total transcript counts were still considerably higher in the FL fraction (Figure 5c). The taxonomic identities of *narG* transcripts spanned a wide phylogenetic range (Figure 5d), with sequences related to anammox bacteria and candidate divisions OP3 and OP1 particularly highly represented in both fractions, which is consistent with results from ETSP OMZ metagenomes (Ganesh *et al.*, 2014). The distribution of *narG* suggests that declines in nitrate reduction after filtration were likely driven primarily by the removal of particulate organic matter (OM) for use by diverse FL nitrate reducers and to a minor extent by the removal of particle-attached nitrate reducers.

Rates of N_2 production by denitrification also declined significantly (by 85%) following particle removal. Transcripts encoding enzymes for nitrite reduction (*nirK/S*) and N_2O and N_2 gas production (*nosZ* and *norB*, respectively) were at low abundance compared with those of nitrate reduction and anammox (Figure 5c), and showed contrasting size fraction distributions. Transcripts for NirK/S were at relatively uniform proportional abundances in PA and FL data sets. These transcripts reflected a diverse assemblage, but were notably enriched at the lower oxycline and oxic–nitrite interface by Thaumarchaeota *nirK* sequences (Figure 5d). NO-forming Nir activity in ammonia-oxidizing Thaumarchaeota is not well understood (Lund *et al.*, 2012), but may have roles in both energy generation and nitrite detoxification, with the latter of potential relevance in nitrite-replete OMZs. In contrast, *nosZ* and *norB* transcripts were enriched up to 28-fold in PA fractions, particularly at upper OMZ depths (Figure 5b), and affiliated with a community taxonomically distinct from that catalyzing upstream steps of denitrification (Figure 5d), as also reported in Dalsgaard *et al.* (2014). These results support metagenome data from the Chilean OMZ (Ganesh *et al.*, 2014) and from an estuarine site (Smith *et al.*, 2013) showing *nor/nos* enrichment in PA fractions, suggesting a conserved PA niche. After scaling based on 16S gene counts (a proxy for cell counts), absolute counts of *nosZ* and

Figure 5 Measured rates and marker gene transcript levels for major dissimilatory N cycle processes. Process rates (a) are shown for incubations with particles (no filtration) and without particles measuring $1.6 \mu\text{m}$ or larger. Zero values indicate non-significant rates and error bars represent the standard errors. Note variation in y axis scales. (b) Marker gene transcript abundances in FL (0.2–1.6 μm) and PA (1.6–30 μm) filter fractions. Abundances are calculated as read count per gene per kilobase of gene length, and shown as a proportion of the abundance of transcripts matching the universal, single-copy gene *rpoB*. A value of 1 indicates abundance equal to that of *rpoB*. Note variation in y axis scales. (c) Multiplies the values in b by the counts of bacterial 16S genes in Figure 1f and the FL/PA ratio (for FL counts only), with the values then divided by 1 000 000 for presentation. The resulting values do not reflect absolute counts, but provide an approximation of how variation in bacterial abundance (inferred by proxy from 16S counts) is predicted to affect comparisons of absolute transcript counts across samples, assuming that absolute transcript counts scale with bacterial load. Scaled *amoC* values are not provided in c, as FL:PA ratios were determined using bacterial-specific primers, and *amoC* transcripts were dominated exclusively by archaeal sequences; FL:PA ratios do not reflect archaeal contributions. Patterns in c should be interpreted cautiously, as they could change if RNA content per unit biomass varies substantially among samples. (d) The taxonomic affiliations of marker gene transcripts based on NCBI annotations of genes identified as top matches ($>$ bit score 50) via BLASTX.

norB transcripts were estimated to be comparable between size fractions (Figure 5c), suggesting that filtration removes a significant proportion of the N₂O- and N₂-forming denitrifier community.

Anammox. Anammox rates declined 53–100% without particles. These declines may indicate that particle removal eliminates an important substrate source for FL anammox bacteria. Particles could facilitate



anammox by providing (1) ammonium remineralized by heterotrophic PA bacteria consuming particulate OM (Shanks and Trent, 1979), (2) ammonium produced by anammox bacteria via oxidation of particulate OM with nitrate or nitrite (Kartal *et al.*, 2007) or (3) nitrite produced by other (non-anammox) nitrate-reducing heterotrophs consuming particulate OM. Explanations (1) and (3) are consistent with the observed reduction in rates of nitrate reduction to nitrite, the most active respiratory process detected, in the absence of particles. We therefore hypothesize that particle-dependent nitrate or nitrite reduction by both FL and PA communities likely provides a critical supply of ammonium or nitrite for anammox, although it remains unclear whether anammox bacteria are ammonium- or nitrite-limited in OMZs (Lam and Kuypers, 2011; De Brabandere *et al.*, 2014).

Two alternate hypotheses could explain the decline in anammox after filtration. First, filtration removed a significant fraction of total anammox-capable cells. This hypothesis is dismissed given the substantial enrichments of total 16S rRNA gene copies and Brocadiales 16S copies in the FL fraction. Second, anammox-capable cells in PA fractions, although a minor component of the total population, contributed disproportionately to bulk anammox rates, potentially overexpressing anammox enzymes compared with FL cells. The active transcription of anammox genes in the FL fraction argues against this hypothesis. Transcripts encoding hydrazine oxidoreductase, catalyzing hydrazine oxidation to N₂ during anammox, were up to 15-fold higher in proportional abundance in FL samples (Figure 5b), consistent with the 14-fold enrichment of Brocadiales 16S genes in the FL fraction.

To further examine the potential that anammox bacteria alter their metabolism between FL and PA niches, we tested for differential gene expression between PA and FL data sets, focusing only on genes from known anammox genera (Supplementary Methods). After normalizing for variation in total transcripts matching anammox genera, PA and FL transcript profiles were well correlated ($R^2 = 0.81$) and no genes (of 1392 total) were differentially expressed between fractions ($P > 0.05$). However, testing for DE required grouping data sets from different depths as replicates, raising the possibility that depth-specific variation confounded the detection of DE between fractions. Despite this apparent uniformity in expression, marker genes for the anammox process itself (*hzo* and *hzs* encoding hydrazine synthase) were consistently, although not statistically, enriched (2–3 fold) in the FL fraction, suggesting an upregulation of anammox in the FL niche (Supplementary Figure S5). In contrast, transcripts encoding nitrate reductase NarGH were among those most abundant and enriched in PA profiles. Nar likely acts in reverse in anammox bacteria, converting nitrite to nitrate and helping replenish electrons lost during CO₂ fixation via the acetyl-CoA pathway (Strous *et al.*, 2006; Jetten *et al.*,

2009). Here transcripts encoding key acetyl-CoA pathway genes (formate dehydrogenase and carbon monoxide dehydrogenase) were ~10-fold less abundant than Nar transcripts, and did not differ appreciably between PA and FL fractions. Alternatively, Nar in anammox bacteria may function as a traditional nitrate reductase during anaerobic growth on organic compounds (Güven *et al.*, 2005), and it is plausible that oxidation of organics is enhanced in anammox bacteria on particles. The observed fold change differences in *hzo*, *hzs* and *nar* raise the possibility of microniche-specific gene expression by anammox-capable bacteria, but do not support the hypothesis that the anammox process itself is upregulated in PA compared with FL communities. Thus, the effect of filtration on anammox rates is best explained by dependence of FL anammox bacteria on the PA fraction for substrate.

Nitrification. Compared with denitrification and anammox, ammonia and nitrite oxidation were less affected by particle removal. Filtration decreased ammonia oxidation rates by ~25% in the lower oxycline and upper OMZ. At the oxic–nitrite interface, rates did not change following filtration. Nitrite oxidation decreased by ~50% without particles, although rates after filtration were still several orders of magnitude higher than those of other N processes. Transcripts encoding ammonia monooxygenase (*amoC*) were proportionately enriched in the FL fraction (excluding at 85 m) and affiliated predominantly with sequences annotated as Thaumarchaeota or as ‘uncultured crenarchaeote’ (the latter were entered into NCBI before formal recognition of the ‘Thaumarchaeota’ designation and likely should be re-annotated as Thaumarchaeota; Figure 5d). Transcripts encoding nitrite oxidoreductase (*nxrB*) did not show a strong size fraction-specific enrichment, consistent with *nxrB* gene distributions in metagenomes from the Chilean OMZ (Ganesh *et al.*, 2014). *NxrB* transcripts affiliated primarily with sequences from the genome of *Nitrospina gracilis* (Lücker *et al.*, 2013), supporting reports of high *Nitrospina* activity in the ETNP region (Beman *et al.*, 2013). Analysis of only *N. gracilis*-affiliated transcripts did not reveal any genes that were differentially expressed between FL and PA fractions ($P > 0.05$), although low *N. gracilis* read counts in PA data sets (5% those in FL data sets) likely confounded statistical detection. Indeed, *nxr* genes (all subunits combined) represented similar proportions of total *N. gracilis* counts in both fractions (2.5% and 3.2% in FL and PA, respectively), suggesting that expression of nitrite oxidation genes was not substantially altered between PA and FL niches.

Conclusions

Filter fractionation significantly altered N metabolism rates, confirming a critical role for particles and

PA microorganisms in OMZ N cycling. A strong dependence on particles may help explain heterogeneity of denitrification and anammox rates among OMZ sites and time points (Dalsgaard *et al.*, 2012; De Brabandere *et al.*, 2014; Kalvelage *et al.*, 2013), notably if particle load varies over depth and distance from shore or between times of high versus low export from the photic zone. Our data also suggest differences in how OMZ microbes interact with particles. A significant fraction of some functional groups, notably N₂O- and N₂-producing denitrifiers, are recovered in PA fractions, suggesting direct adherence to particles, or potentially larger cell sizes. A tight coupling to particle surfaces could facilitate access to organic carbon for respiration, as well as oxidized N compounds produced by upstream steps of the denitrification pathway. Indeed, enhanced hydrolytic activity of particulate organic substrates has been demonstrated in diverse marine waters (Hoppe *et al.*, 1993; Taylor *et al.*, 2009; Yamada *et al.*, 2012). Denitrifiers are generally known as facultative anaerobes (Zumft, 1997) and populations of denitrifiers on OMZ particles may develop during sinking through the oxycline, switching to denitrification upon transition to the OMZ core.

In contrast, groups such as obligately anaerobic anammox bacteria are recovered almost exclusively within the FL fraction, but appear no less dependent on particles. Anammox cells presumably rely on particles indirectly as sources of nitrite and ammonium, produced by nitrate or nitrite reducers consuming particulate OM. Although anammox cells have been recovered in direct contact with particles in other systems (Woebken *et al.*, 2007), enrichment of anammox genes and transcripts in OMZ FL fractions suggests a relatively loose physical association with particles, although it is possible that some particle-adhered cells are dislodged into the FL fraction during filtration. It is plausible that the proportion of the anammox community adhered to particles varies depending on local substrate conditions and oxygen content. Direct adherence may enable access to anoxic microniches and be favored at upper OMZ depths where water column oxygen content is closer to the threshold for anammox inhibition (~900 nM; Dalsgaard *et al.*, 2014).

The potential for OMZ microbes to alter their physiology between FL and PA niches remains unresolved. Anammox Planctomycetes and nitrite-oxidizing *Nitrospina*, two groups recovered in both FL and PA fractions and occupying relatively well-defined functional roles, did not exhibit significantly different expression profiles between fractions. This suggests that the physical act of filtration had a relatively minor effect on cell state. Nonetheless, certain genes exhibited large fold changes in relative abundance between fractions, raising the possibility that additional analyzes with higher replication per depth may reveal size fraction-specific transcriptional differences in certain taxa. Clarifying such patterns, potentially by sequencing deeply across

biological replicates coupled with transcriptome mapping to reference genomes, may help estimate per-cell differences in biochemical processing at the microscale. However, the use of biomass fractionation to characterize the microspatial architecture of microbial activity remains challenging. As shown here, particle removal significantly disrupts bulk N cycle processes mediated by a FL majority, likely by severing important chemical and biological linkages between FL and PA niches.

Conflict of Interest

The authors declare no conflict of interest.

Acknowledgements

We thank the crew of the *R/V New Horizon* for help in sample collection, Neha Sarode and Josh Parris for help in sequencing, Anni Glud for technical assistance and for preparing the STOX, and Peter Girguis, Kathy Barbeau and Forest Rohwer for providing essential equipment. This work was supported by the National Science Foundation (1151698 to FJS), the Sloan Foundation (RC944 to FJS), the Danish National Research Foundation DNR53, the Danish Council of Independent Research and the European Research Council 'Oxygen' grant (267233 supporting LAB, ML and BT).

References

- Babbitt AR, Keil RG, Devol AH, Ward BB. (2014). Organic matter stoichiometry, flux, and oxygen control nitrogen loss in the ocean. *Science* **344**: 406–408.
- Beman JM, Popp BN, Alford SE. (2012). Quantification of ammonia oxidation rates and ammonia-oxidizing archaea and bacteria at high resolution in the Gulf of California and eastern tropical North Pacific Ocean. *Limnol Oceanogr* **57**: 711–726.
- Beman JM, Carolan MT. (2013). Deoxygenation alters bacterial diversity and community composition in the ocean's largest oxygen minimum zone. *Nat Commun* **4**: 2705.
- Beman JM, Leilei Shih J, Popp BN. (2013). Nitrite oxidation in the upper water column and oxygen minimum zone of the eastern tropical North Pacific Ocean. *ISME J* **7**: 2192–2205.
- Blazewicz SJ, Barnard RL, Daly RA, Firestone MK. (2013). Evaluating rRNA as an indicator of microbial activity in environmental communities: limitations and uses. *ISME J* **7**: 2061–2208.
- Campbell BJ, Yu L, Heidelberg JF, Kirchman DL. (2011). Activity of abundant and rare bacteria in a coastal ocean. *Proc Natl Acad Sci USA* **108**: 12776–12781.
- Canfield DE, Stewart FJ, Thamdrup B, De Brabandere L, Dalsgaard T, Delong EF *et al.* (2010). A cryptic sulfur cycle in oxygen-minimum-zone waters off the Chilean coast. *Science* **330**: 1375–1378.
- Caporaso JG, Kuczynski J, Stombaugh J, Bittinger K, Bushman FD, Costello EK *et al.* (2010). QIIME allows analysis of high-throughput community sequencing data. *Nat Methods* **7**: 335–336.

- Caporaso JG, Lauber CL, Walters WA, Berg-Lyons D, Lozupone CA, Turnbaugh PJ *et al.* (2011). Global patterns of 16 S rRNA diversity at a depth of millions of sequences per sample. *Proc Natl Acad Sci USA* **15**: 108.
- Ceja-Navarro JA, Nguyen NH, Karaoz U, Gross SR, Herman DJ, Andersen GL *et al.* (2014). Compartmentalized microbial composition, oxygen gradients and nitrogen fixation in the gut of *Odontotaenius disjunctus*. *ISME J* **8**: 6–18.
- Cho BC, Azam F. (1988). Major role of bacteria in biogeochemical fluxes in the ocean's interior. *Nature* **332**: 441–443.
- Cline JD, Richards FA. (1974). Oxygen deficient conditions and nitrate reduction in the eastern tropical North Pacific ocean. *Limnol Oceanogr* **17**: 885–900.
- Codispoti LA, Brandes JA, Christensen JP, Devol AH, Naqvi SWA, Paerl HW *et al.* (2001). The oceanic fixed nitrogen and nitrous oxide budgets: moving targets as we enter the anthropocene? *Sci Mar* **65**: 85–105.
- Dalsgaard T, Thamdrup B, Farias L, Revsbech NP. (2012). Anammox and denitrification in the oxygen minimum zone of the eastern South Pacific. *Limnol Oceanogr* **57**: 1331–1346.
- Dalsgaard T, Stewart FJ, Thamdrup B, De Brabandere L, Revsbech NP, Ulloa O *et al.* (2014). Oxygen at nanomolar levels reversibly suppresses process rates and gene expression of anammox and denitrification in the oxygen minimum zone off northern Chile. *mBio* **5**: e01966–14.
- De Brabandere L, Canfield DE, Dalsgaard T, Friederich GE, Revsbech NP, Ulloa O *et al.* (2014). Vertical partitioning of nitrogen-loss processes across the oxic–anoxic interface of an oceanic oxygen minimum zone. *Environ Microbiol* **16**: 3041–3054.
- DeLong EF, Franks DG, Alldredge AL. (1993). Phylogenetic diversity of aggregate-attached vs free-living marine bacterial assemblages. *Limnol Oceanogr* **38**: 924–934.
- DeSantis TZ, Hugenholtz P, Larsen N, Rojas M, Brodie EL, Keller K *et al.* (2006). Greengenes, a chimera-checked 16 S rRNA gene database and workbench compatible with ARB. *Appl Environ Microbiol* **72**: 5069–5072.
- Edgar RC. (2010). Search and clustering orders of magnitude faster than BLAST. *Bioinformatics* **26**: 2460–2461.
- Eldholm V, Norheim G, von der Lippe B, Kinander W, Dahle UR, Caugant DA *et al.* (2014). Evolution of extensively drug-resistant *Mycobacterium tuberculosis* from a susceptible ancestor in a single patient. *Genome Biol* **15**: 490.
- Faith DP. (1992). Conservation evaluation and phylogenetic diversity. *Biol Conserv* **61**: 1–10.
- Frias-Lopez J, Shi Y, Tyson GW, Coleman ML, Schuster SC, Chisholm SW *et al.* (2008). Microbial community gene expression in ocean surface waters. *Proc Natl Acad Sci USA* **105**: 3805–3810.
- Fuchsman CA, Staley JT, Oakley BB, Kirkpatrick JB, Murray JW. (2012). Free-living and aggregate-associated Planctomycetes in the Black Sea. *FEMS Microbiol Ecol* **80**: 402–416.
- Füssel J, Lam P, Lavik G, Jensen MM, Holtappels M, Gunter M *et al.* (2012). Nitrite oxidation in the Namibian oxygen minimum zone. *ISME J* **6**: 1200–1209.
- Ganesh S, Parris DJ, DeLong EF, Stewart FJ. (2014). Metagenomic analysis of size-fractionated picoplankton in a marine oxygen minimum zone. *ISME J* **8**: 187–211.
- Ghiglione JF, Conan P, Pujo-Pay M. (2009). Diversity of total and active free-living vs particle-attached bacteria in the euphotic zone of the NW Mediterranean Sea. *FEMS Microbiol Lett* **299**: 9–21.
- Grossart HP, Hietanen S, Ploug H. (2003). Microbial dynamics on diatom aggregates in Øresund, Denmark. *Mar Ecol Prog Ser* **249**: 69–78.
- Grossart HP, Tang KW, Kjørboe T, Ploug H. (2007). Comparison of cell-specific activity between free-living and attached bacteria using isolates and natural assemblages. *FEMS Microbiol Lett* **266**: 194–200.
- Gruber N. The dynamics of the marine nitrogen cycle and its influence on atmospheric CO₂ variations. Follows M, Oguz T. *The Ocean Carbon Cycle and Climate, NATO ASI Series*. Kluwer: Dordrecht, Germany, 2004; 97–148.
- Güven D, Dapena A, Kartal B, Schmid MC, Maas B, van de Pas-Schoonen K *et al.* (2005). Propionate oxidation by and methanol inhibition of anaerobic ammonium-oxidizing bacteria. *Appl Environ Microbiol* **71**: 1066–1071.
- Hardcastle TJ, Kelly KA. (2010). baySeq: Empirical Bayesian methods for identifying differential expression in sequence count data. *BMC Bioinform* **11**: 422.
- Hatt JK, Ritalahti KM, Ogles DM, Lebrón CA, Löffler FE. (2013). Design and application of an internal amplification control to improve *Dehalococcoides mccartyi* 16 S rRNA gene enumeration by qPCR. *Environ Sci Technol* **47**: 11131–11138.
- Hollibaugh T, Wong PS, Murrell MC. (2000). Similarity of particle-associated and free-living bacterial communities in northern San Francisco Bay, California. *Aquat Microb Ecol* **21**: 102–114.
- Hoppe HG, Ducklow H, Karrasch B. (1993). Evidence for dependency of bacterial growth on enzymatic hydrolysis of particulate organic matter in the mesopelagic ocean. *Mar Ecol Prog Ser* **93**: 277–283.
- Hunt DE, David LA, Gevers D, Preheim SP, Alm EJ, Polz MF *et al.* (2008). Resource partitioning and sympatric differentiation among closely related bacterioplankton. *Science* **320**: 1081–1085.
- Hunt DE, Lin Y, Church MJ, Karl DM, Tringe SG, Izzo LK *et al.* (2013). Relationship between abundance and specific activity of bacterioplankton in open ocean surface waters. *Appl Environ Microbiol* **79**: 177–184.
- Huson DH, Mitra S, Ruscheweyh HJ, Weber N, Schuster SC. (2011). Integrative analysis of environmental sequences using MEGAN4. *Genome Res* **21**: 1552–1560.
- Ivars-Martinez E, Martin-Cuadrado AB, D'Auria G, Mira A, Ferreria S, Johnson J *et al.* (2008). Comparative genomics of two ecotypes of the marine planktonic copiotroph *Alteromonas macleodii* suggests alternative lifestyles associated with different kinds of particulate organic matter. *ISME J* **2**: 1194–1212.
- Jetten MS, Niftrik LV, Strous M, Kartal B, Keltjens JT, Op den Camp HJ *et al.* (2009). Biochemistry and molecular biology of anammox bacteria. *Crit Rev Biochem Mol Biol* **44**: 65–84.
- Kalvelage T, Lavik G, Lam P, Contreras S, Arteaga L, Loscher CR *et al.* (2013). Nitrogen cycling driven by organic matter export in the South Pacific oxygen minimum zone. *Nat Geosci* **6**: 228–234.
- Karl DM, Knauer GA, Martin JH. (1988). Downward flux of particulate organic matter in the ocean: a particle decomposition paradox. *Nature* **332**: 438–441.

- Karstensen J, Stramma L, Visbeck M. (2008). Oxygen minimum zones in the eastern tropical Atlantic and Pacific oceans. *Prog Oceanogr* **77**: 331–350.
- Kartal B, Kuypers MMM, Lavik G, Schalk J, Op den Camp HJM, Jetten MSM *et al.* (2007). Anammox bacteria disguised as denitrifiers: nitrate reduction to dinitrogen gas via nitrite and ammonium. *Environ Microbiol* **9**: 635–642.
- Kong L, Jing H, Kataoka T, Buchwald C, Liu H. (2013). Diversity and spatial distribution of hydrazine oxidoreductase (hzo) gene in the oxygen minimum zone off Costa Rica. *PLoS One* **8**: e78275.
- Kozich JJ, Westcott SL, Baxter NT, Highlander SK, Schloss PD. (2013). Development of a dual-index sequencing strategy and curation pipeline for analyzing amplicon sequence data on the MiSeq Illumina sequencing platform. *Appl Environ Microbiol* **79**: 5112–5120.
- Lam P, Lavik G, Jensen MM, van de Vossenberg J, Schmid M, Woebken D *et al.* (2009). Revising the nitrogen cycle in the Peruvian oxygen minimum zone. *Proc Natl Acad Sci USA* **106**: 4752–4757.
- Lam P, Kuypers MMM. (2011). Microbial nitrogen cycling processes in oxygen minimum zones. *Annu Rev Mar Sci* **3**: 317–345.
- Lozupone C, Knight R. (2005). UniFrac: a new phylogenetic method for comparing microbial communities. *Appl Environ Microb* **71**: 8228–8235.
- Lücker S, Nowka B, Rattei T, Spieck E, Daims H. (2013). The genome of *Nitrospina gracilis* illuminates the metabolism and evolution of the major marine nitrite oxidizer. *Front Microbiol* **4**: 27.
- Lund MB, Smith JM, Francis CA. (2012). Diversity, abundance and expression of nitrite reductase (*nirK*)-like genes in marine thaumarchaea. *ISME J* **6**: 1966–1977.
- Mcllvin MR, Altabet MA. (2005). Chemical conversion of nitrate and nitrite to nitrous oxide for nitrogen and oxygen isotopic analysis in freshwater and seawater. *Anal Chem* **77**: 5589–5595.
- Milohanic E, Glaser P, Coppée JY, Frangeul L, Vega Y, Vázquez-Boland JA *et al.* (2003). Transcriptome analysis of *Listeria monocytogenes* identifies three groups of genes differently regulated by PrfA. *Mol Microbiol* **47**: 1613–1625.
- Naqvi SWA, Kumar MD, Narvekar PV, De Sousa SN, George MD, Silva CD *et al.* (1993). An intermediate nepheloid layer associated with high microbial rates and denitrification in the northwest Indian Ocean. *J Geophys Res* **98**: 16469–16479.
- Paulmier A, Ruiz Pino. (2009). Oxygen minimum zones (OMZs) in the modern ocean. *Prog Oceanogr* **80**: 113–128.
- Podlaska A, Wakeham SG, Fanning KA, Taylor GT. Microbial community structure and productivity in the oxygen minimum zone of the eastern tropical North Pacific. *Deep Sea Res Part I* 2012; **66**: 77–89.
- Rao D, Webb JS, Kjelleberg S. (2005). Competitive interactions in mixed-species biofilms containing the marine bacterium *Pseudoalteromonas tunicata*. *Appl Environ Microbiol* **71**: 1729–1736.
- Revsbech NP, Larsen LH, Gundersen J, Dalsgaard T, Ulloa O, Thamdrup B *et al.* (2009). Determination of ultra-low oxygen concentrations in oxygen minimum zones by the STOX sensor. *Limnol Oceanogr Methods* **7**: 371–381.
- Ritalahti KM, Amos BK, Sung Y, Wu Q, Koenigsberg SS, Löffler FE *et al.* (2006). Quantitative PCR targeting 16S rRNA and reductive dehalogenase genes simultaneously monitors multiple *Dehalococcoides* strains. *Appl Environ Microbiol* **72**: 2765–2774.
- Rush D, Wakeham SG, Hopmans EC, Schouten S, Sinninghe Damsté JS. (2012). Biomarker evidence for anammox in the oxygen minimum zone of the Eastern Tropical North Pacific. *Org Geochem* **53**: 80–87.
- Satinsky BM, Crump BC, Smith CB, Sharma S, Zielinski BL, Doherty M *et al.* (2014). Microspatial gene expression patterns in the Amazon River Plume. *Proc Natl Acad Sci USA* **111**: 11085–11090.
- Schmieder R, Lim YW, Edwards R. (2012). Identification and removal of ribosomal RNA sequences from metatranscriptomes. *Bioinformatics* **28**: 433–435.
- Schumann U, Edwards MD, Rasmussen T, Bartlett W, van West P, Booth IR *et al.* (2010). YbdG in *Escherichia coli* is a threshold-setting mechanosensitive channel with MscM activity. *Proc Natl Acad Sci USA* **107**: 12664–12669.
- Shanks AL, Trent JD. (1979). Marine snow: microscale nutrient patches. *Limnol Oceanogr* **24**: 850–854.
- Sheik CS, Jain S, Dick GJ. (2014). Metabolic flexibility of enigmatic SAR324 revealed through metagenomics and metatranscriptomics. *Environ Microbiol* **6**: 304–317.
- Sihto HM, Tasara T, Stephan R, Johler S. (2014). Validation of reference genes for normalization of qPCR mRNA expression levels in *Staphylococcus aureus* exposed to osmotic and lactic acid stress conditions encountered during food production and preservation. *FEMS Microbiol Lett* **356**: 134–140.
- Simon M, Grossart HP, Schweitzer B, Ploug H. (2002). Microbial Ecology of organic aggregates in aquatic ecosystems. *Aquat Microb Ecol* **28**: 175–211.
- Smith MW, Allen LZ, Allen AE, Herfort L, Simon HM. (2013). Contrasting genomic properties of free-living and particle-attached microbial assemblages within a coastal ecosystem. *Front Microbiol* **4**: 120.
- Spinrad RW, Glover H, Ward BB, Codispoti LA, Kullenberg G. (1989). Suspended particle and bacterial maxima in Peruvian coastal waters during a cold water anomaly. *Deep-Sea Res* **36**: 715–733.
- Stewart FJ, Ulloa O, DeLong EF. (2012). Microbial metatranscriptomics in a permanent marine oxygen minimum zone. *Environ Microbiol* **14**: 23–40.
- Stocker R. (2012). Marine microbes see a sea of gradients. *Science* **338**: 628–633.
- Storey JD, Tibshirani R. (2003). Statistical significance for genomewide studies. *Proc Natl Acad Sci USA* **100**: 9440–9445.
- Strous M, Pelletier E, Mangenot S, Rattei T, Lehner A, Taylor MW *et al.* (2006). Deciphering the evolution and metabolism of an anammox bacterium from a community genome. *Nature* **440**: 790–794.
- Sue D, Fink D, Wiedmann M, Boor KJ. (2004). Sigma(B)-dependent gene induction and expression in *Listeria monocytogenes* during osmotic and acid stress conditions simulating the intestinal environment. *Microbiology* **150**: 3843–3855.
- Swan BK, Martinez-Garcia M, Preston CM, Sczyrba A, Woyke T, Lamy D *et al.* (2011). Potential for chemolithoautotrophy among ubiquitous bacteria lineages in the dark ocean. *Science* **333**: 1296–1300.
- Taylor GT, Thunell R, Varela R, Benitez-Nelson C, Scranton MI. (2009). Hydrolytic ectoenzyme activity associated with suspended and sinking organic particles within the anoxic Cariaco Basin. *Deep Sea Res I* **56**: 1266–1283.

- Teske A, Alm E, Regan JM, Toze S, Rittmann BE, Stahl DA *et al.* (1994). Evolutionary relationships among ammonia- and nitrite-oxidizing bacteria. *J Bacteriol* **176**: 6623–6630.
- Thamdrup B, Dalsgaard T. (2002). Production of N₂ through anaerobic ammonium oxidation coupled to nitrate reduction in marine sediments. *Appl Environ Microbiol* **68**: 1312–1318.
- Thamdrup B, Dalsgaard T, Jensen MM, Ulloa O, Farias L, Escribano R *et al.* (2006). Anaerobic ammonium oxidation in the oxygen-deficient waters off northern Chile. *Limnol Oceanogr* **51**: 2145–2156.
- Tiano L, Garcia Robledo E, Dalsgaard T, Devol A, Ward B, Ulloa O *et al.* (2014). Oxygen distribution and aerobic respiration in the north and southeastern tropical Pacific oxygen minimum zones. *Deep-Sea Res I* **194**: 173–183.
- Turley CM, Stutt ED. (2000). Depth-related cell-specific bacterial leucine incorporation rates on particles and its biogeochemical significance in the Northwest Mediterranean. *Limnol Oceanogr* **45**: 419–425.
- Ulloa O, Canfield DE, DeLong EF, Letelier RM, Stewart FJ. (2012). Perspective: microbial oceanography of anoxic oxygen minimum zones. *Proc Natl Acad Sci USA* **109**: 15996–16003.
- Vandecasteele SJ, Peetermans WE, Merckx R, Van Eldere J. (2001). Quantification of expression of *Staphylococcus epidermidis* housekeeping genes with Taqman quantitative PCR during in vitro growth and under different conditions. *J Bacteriol* **183**: 7094–7101.
- Walsh DA, Zaikova E, Howes CG, Song YC, Wright JJ, Tringe SG *et al.* (2009). Metagenome of a versatile chemolithoautotroph from expanding oceanic dead zones. *Science* **326**: 578–582.
- Whitmire AL, Letelier RM, Villagran V, Ulloa O. (2009). Autonomous observations of in vivo fluorescence and particle backscattering in an oceanic oxygen minimum zone. *Optics Express* **17**: 21992–22004.
- Woebken D, Fuchs BM, Kuypers MM, Amann R. (2007). Potential interactions of particle-associated anammox bacteria with bacterial and archaeal partners in the Namibian upwelling system. *Appl Environ Microbiol* **73**: 4648–4657.
- Wright JJ, Konwar KM, Hallam SJ. (2012). Microbial ecology of expanding oxygen minimum zones. *Nat Rev Microbiol* **10**: 381–394.
- Wright JJ, Mewis K, Hanson NW, Konwar KM, Maas KR, Hallam SJ *et al.* (2014). Genomic properties of Marine Group A bacteria indicate a role in the marine sulfur cycle. *ISME J* **8**: 455–468.
- Yamada N, Fukuda H, Ogawa H, Saito H, Suzumura M. (2012). Heterotrophic bacterial production and extracellular enzymatic activity in sinking particulate matter in the western North Pacific Ocean. *Front Microbiol* **3**: 379.
- Zumft WG. (1997). Cell biology and molecular basis of denitrification. *Microbiol Mol Biol Rev* **61**: 533–616.

Supplementary Information accompanies this paper on The ISME Journal website (<http://www.nature.com/ismej>)